International Journal of Coal Science & Technology (2025) 12:74
https://doi.org/10.1007/s40789-025-00805-1

RESEARCH

Oiliness gradation of hybrid sedimentary shale with low-moderate organic matter content: a case study of the Paleocene Shahejie Formation in Dongpu Depression, Bohai Bay Basin

Zhiming Xiong[1,2] · Tao Hu[1,2] · Yuqi Wu[1,2] · Yunlong Xu[3] · Jiyou Fu[4] · Huiyi Xiao[1,2] · Yuan Liu[1,2] · Kuo Zhou[1,2] · Qinglong Lei[1,2] · Tianshun Chen[1,2] · Xiaofei Lin[1,2] · Mingxing Liu[1,2] · Shu Jiang[5] · Maowen Li[6]

Received: 3 January 2025 / Revised: 27 March 2025 / Accepted: 9 May 2025

Abstract

Shale oil resources are abundant on Earth, of which hybrid sedimentary shale (HSS) oil is an important component, including high and medium–low organic matter content (TOC). Oil content, especially the oiliness gradation, is a key parameter for shale oil evaluation and numerous studies had been conducted. However, most studies concentrated on the HSS with high TOC, making oil content evaluation of the HSS with medium–low TOC challenging. The Paleocene Shahejie Formation (E_2s) shale in Dongpu Depression is a typical HSS with low-moderate TOC, showing great shale oil resource potential. Integrated geochemical characterization of 270 core samples were conducted and results show that, the E_2s shale has fair-good hydrocarbon generation potential, with TOC ranging from 0.06% to 3.6% (Avg. 0.86%) and II_1–II_2 kerogen type in thermally mature. The hydrocarbon generation potential decreases with kerogen types changing from type I to III, but S_{1C} and the oil saturation index (OSI) (S_1*100/TOC > 100) increase from type I to II_1, and then decrease from type II_2 to III, indicating shale with type II_2 kerogen have the greatest oil content. This is related to the differences in hydrocarbon expulsion efficiency caused by differential hydrocarbon generation potential and pore-microfractures evolution among shales with different kerogen types. Significant oil micro-migration occurred in E_2s shale, with micro-migration quantity (ΔQ) ranging from − 846 to 993 mg/g (Avg. − 120 mg/g), and 90% and 10% shale exhibit hydrocarbon intra-micro-migration (ΔQ < 0) and extra-micro-migration (ΔQ > 0). The shale with type II_2 kerogen has the greatest intra-micro-migration. Based on S_{1C}, TOC and OSI values and their evolution pattern, shale oil resources were classified into enriched, moderately enriched, less efficient and invalid resources, accounting for 11%, 53%, 16% and 21% respectively, with S_{1C} thresholds of 3.5 and 0.5 mg/g, OSI threshold of 100 mg/g. Compared with previous grading criteria, the gradation criterion established in this study is relatively lower, which is mainly due to the lower TOC and clay mineral content in HSS. Enriched and moderately enriched resources are mainly shales with type II_2 kerogen, followed by type II_1 kerogen, and the $E_2s_4^U$ and $E_2s_3^L$ shale are the most favorable targets for further shale oil exploration. The established oiliness gradation criteria are applicable for the HSS with TOC in other parts of the world.

Keywords Hybrid sedimentary shale · Shale oil · Oiliness · Low-moderate organic matter content · Micro-migration · Grading evaluation criteria

1 Introduction

The shale oil and gas revolution has transformed the global energy landscape, promoting energy independence and significantly boosting oil and gas production in several countries, including the United States (Moine et al. 2016; Milkov 2015; Pang et al. 2023). Global shale oil resources are abundant, with with high organic matter abundance and medium–low organic matter abundance HSS oil being a significant component (Siddiqui et al. 2018; Hu et al. 2022). High organic matter abundance HSS is typified by the Eagle Ford Shale (Altawati et al. 2021) and the E_2s shale in the Jiyang Depression (Teng et al. 2022). Medium–low organic matter abundance HSS includes the Fengcheng Formation shale in the Mahu Sag, Junggar Basin (Jiang et al. 2023), the Lower Ganchaigou Formation shale in the Yingxiongling Depression, Qaidam Basin

Extended author information available on the last page of the article

Published online: 28 July 2025

(Li et al. 2022), and the E_2s in the Dongpu Depression, Bohai Bay Basin (Jiang et al. 2022). Both Types possess substantial potential for shale oil exploration.

Oil content is a key parameter in shale oil evaluation, and previous studies have established various grading evaluation criteria for oil content (Hu et al. 2018a). Jarvie proposed that the oil saturation index (OSI) (S_1*100/TOC > 100) can serve as a threshold for the adsorptive capacity of source rocks, to evaluate potential movable oil content (Jarvie 2012). However, when the absolute values of S_1 and TOC are relatively low, the OSI value may still be high, leading to uncertainties in assessing shale oil potential. Zhang et al. integrated factors such as TOC, R_o, area, burial depth, and thickness, classifying resources into three tiers: prospective, favorable, and core areas (Zhang et al. 2012). However, this method can only provide qualitative assessment due to the data complexity and grading evaluation criteria absence. Lu et al. established a "tripartition" method for oil content evaluation using S_1 and TOC in the southern Songliao Basin, defining boundaries at TOC values of 0.8% and 1.8% to classify shale oil resources into three categories (Lu et al. 2012). This method addresses the limitations of evaluating source rocks solely using the OSI index. However, when TOC is relatively low, the OSI of some samples may be relatively high, potentially leading to inaccurate grading. Li et al. utilized an enhanced ΔlogR model to evaluate the organic matter abundance of the Bakken Shale and discussed the resource potential of the Upper and Lower Bakken shale oil resources. This method relies on TOC calculated using the ΔlogR model, which may lack accuracy (Li et al. 2015a). Li et al. improved the grading evaluation method for argillaceous dolomite shale oil resources by integrating logging data, though it is limited to classifying dolostone (Li et al. 2015b). Li et al. evaluated shale oil potential using a new free hydrocarbon index. However, this method can only qualitatively identify the expulsion and migration of oil and gas, lacking the ability to classify resource potential levels detailed (Li et al. 2016). Hu et al. established a new grading evaluation criteria for shale oil using thresholds of S_1/TOC = 1, TOC = 1%, and TOC = 3.4% to classifying the shale oil resources of the Luchagou Formation in the Junggar Basin into 4 categories (Hu et al. 2018a). Previous studies employed the pyrolysis parameter S_1 and chloroform asphalt "A" to represent the content of residual oil for shale oil evaluation (Jiang et al. 2016). However, light hydrocarbons may be lost during the collection, transportation, and storage before pyrolysis analysis, leading to errors in the shale oil content evaluation. Gong et al. established a light hydrocarbon calibration using the thresholds of S_1/TOC = 2.2, TOC = 0.8% and TOC = 2.9% for assessing the resource potential in the Zhanhua Depression, Bohai Bay basin (Gong et al. 2021). However, this criteria only applies to shale formations with high organic matter abundance. Zhao et al. introduced the calculated parameter movable oil content ($S_{movable}$) to calibrate S_1 and movable oil, yet they continued to employ previous grading evaluation criteria (Xian et al. 2021). Shao et al. conducted a grading evaluation of shale oil in the Qiankou Formation of the Songliao Basin, and highlight the differences in resource quantity before and after light hydrocarbon calibration (Shao et al. 2024). Wang et al. proposed a three-dimensional shale oil evaluation model based T_{max} and oil mobility threshold (OMT) at different thermal maturity levels. This work represents an improvement on the shale oil content evaluation model by Hu et al., but the complexity of model limit its broad application (Hu et al. 2018a; Wang et al. 2022). Therefore, while there is a significant lack of research on the grading evaluation of oil content in HSS with low-moderate organic matter. Further studies are needed to establish a grading evaluation criteria for HSS with low-moderate organic matter abundance.

In this study, 270 continuous HSS core samples were selected from the well Wei 457HF of the Shahejie formation in the Dongpu Depression (DD), Bohai Bay Basin. Multiple experiments such as TOC analysis, pyrolysis analysis, fluorescence microscope observation, laser confocal scanning, and the hydrocarbon expulsion potential method were conducted to establish an oil grading evaluation criteria for HSS with low-moderate organic matter abundance established by Hu et al. (2018a). This study provide insights for the exploration and development for global hybrid sedimentary shale with low-moderate organic matter abundance.

2 Geological setting and samples and methods

2.1 Geological setting

The Bohai Bay basins covering an area of approximately 200,000 square kilometers, is a typical oil-generating basin in China (Jiang et al. 2022). The DD is located in the southwest Bohai Bay Basin with an area of about 5300 km^2. The DD is wide in the north and narrow in the south, bounded by the Luxi uplift to the east and the Lankao uplift to the south and the Shenxian Sag to the north and overlying the Neihuang uplift in the west (Figs. 1a–c) (Yang et al. 2022; Zhu et al. 2023). The third member of the Shahejie Formation (E_2s_3) has the widest distribution and the greatest thickness in the study area, and belongs to the semi-deep lake-deep lake deposition. The lithology is mainly gray mud shale, gray siltstone, fine sandstone, and saltpaste rock with unequal thickness (Villalba 2023; Shao et al. 2018).

2.2 Samples

The 270 samples studied were collected from the Wei 457HF Well, with core depths ranging from 3660 to 3800 m. The TOC test requires the removal of inorganic carbon. Treated samples were tested in a LECO CS-230 carbon sulfur analyzer. The samples underwent rock pyrolysis analysis, primarily completed using a Rock–Eval VI pyrolysis instrument equipped with a Flame Ionization Detector (FID) (Tissot et al. 1987). Unextracted rock samples were crushed to 100 mesh after gentle surface cleaning, and about 50 mg/sample were placed in a pyrolysis furnace heated by a standardized warming procedure (25 °C/min) to release hydrocarbons, and in an oxidizing furnace to release carbon dioxide to obtain free hydrocarbons S_1 (mg /g) and pyrolytic hydrocarbons S_2 (mg/g) (Wu et al. 2025a; Yao et al. 2023). The above experiments were performed by the State Key Laboratory of Oil and Gas Resources and Exploration, China University of Petroleum (Beijing). Fluorescence microscope photos and laser confocal experimental scanning data were obtained from Petroleum Geology Experiment Center, Research Institute of Exploration and Development, Sinopec Zhongyuan Oilfield Branch.

2.3 Methods

This study employs the quantitative method for hydrocarbon micro-migration established by Hu et al. (2024a). It was used to assess hydrocarbon micro-migration. Due to variations in structure, climate, sediment provenance, and depth affecting

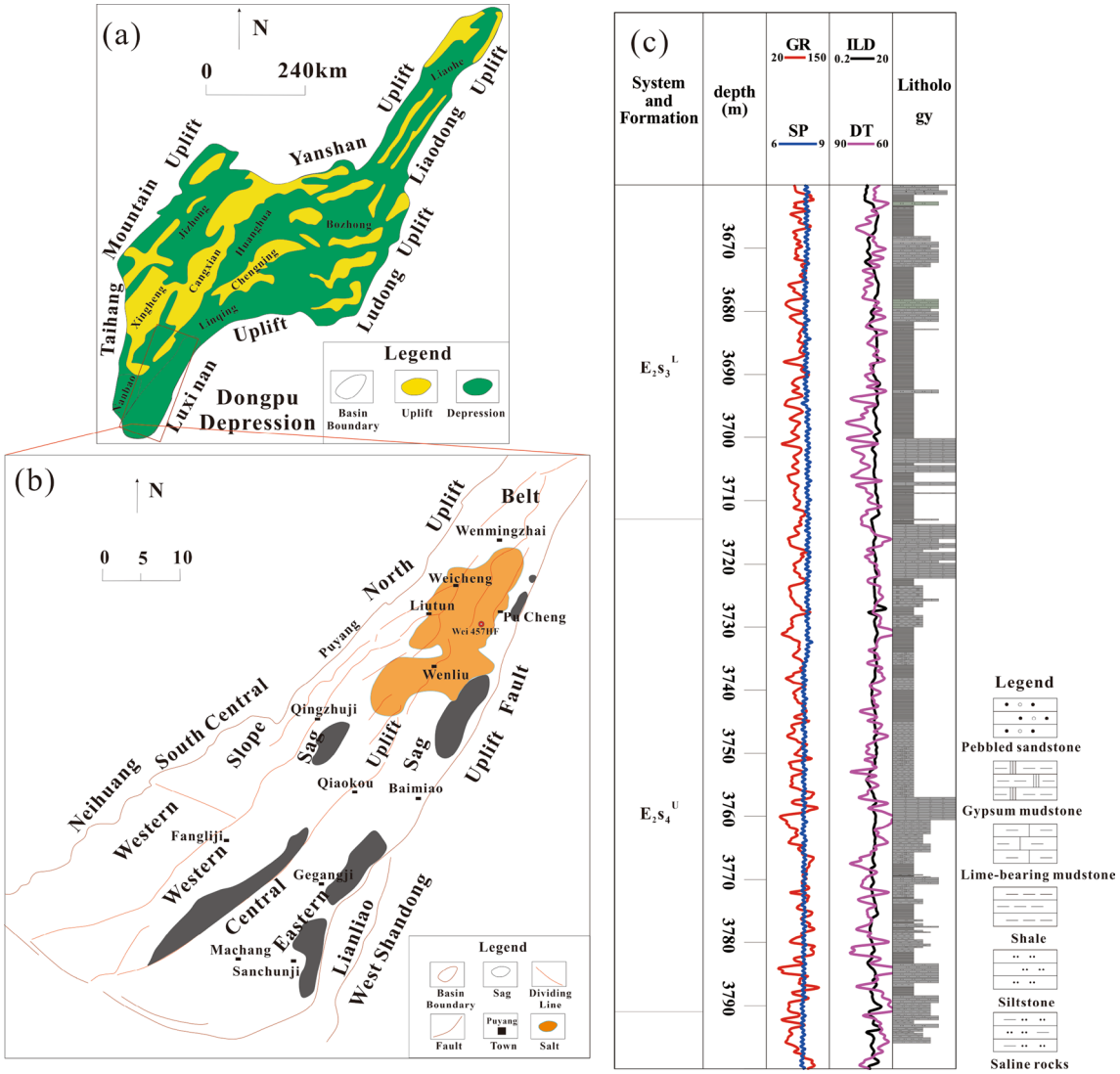

Fig. 1 Geological map of E_2s, DD, Bohai Bay Basin. **a** The location of DD in the Bohai Bay Basin; **b** Distribution of faults (middle of the third member of E_2s) and sags in the DD, modified after (Hu et al. 2021a, b); **c** The formation, depth, logging curves, and lithology of the Well Wei 457HF

sedimentary environment, organic matter input, thermal evolution, and hydrocarbon generation and expulsion, shale exhibits significant heterogeneities in mineral composition, sedimentary structure, organic matter abundance and types. Shales within same stratum at similar depths can exhibit distinct geological and geochemical features, necessitating treatment as independent cells. Variations in mineral composition, sedimentary structure, and organic matter abundance and type lead to differences in hydrocarbon generation and expulsion processes and oil storage capacity, resulting in variable shale oil contents.

Since most pyrolysis data were tested after hydrocarbon expulsion and TOC content changes during thermal evolution, the currently measured hydrocarbon generation potential must be restored to its original state. Kerogen kinetics is important in resource evaluation for better understanding source rock thermal maturation processes, and the relationship between HI and T_{max} demonstrates the kinetic behavior of shales, typically expressed as hydrocarbon transformation ratio. This study utilized the data-driven model to reconstruct the original hydrogen index, representing the original hydrocarbon generation potential, as shown below:

$$H_I = H_I^0 \left\{ 1 - \exp\left[-\left(\frac{T_{\max}}{\beta} \right)^{\theta} \right] \right\} + c \tag{1}$$

$$T_R = \frac{1200}{H_I^0} \frac{\left(H_I^0 - H_I\right)}{\left(1200 - H_I\right)} \tag{2}$$

where H_I^O is the original H_I, mg HC/g TOC; H_I is the hydrogen index (S_2/TOC*100, mg HC/g TOC); T_R is the kerogen transformation rate, %; β and θ are unknown parameters specific to kerogen kinetics; and c is a constant indicating the error magnitude in the measured hydrogen index at very high T_{max}. (Hu et al. 2024a).

The amount of micro-migration hydrocarbon ΔQ shows the amount of externally charged hydrocarbons, which leads to differences in oil content among various hydrocarbon expulsion units. Therefore, there are two cases: (1) $\Delta Q < 0$ exhibits hydrocarbon expulsion phenomenon, and the larger absolute value of ΔQ indicates the larger amount of hydrocarbon expulsion phenomenon; (2) $\Delta Q > 0$ exhibits hydrocarbon charging phenomenon, and the larger absolute value of ΔQ indicates the larger amount of hydrocarbon expulsion phenomenon.

We base our light hydrocarbon recovery on the relationship between light hydrocarbon composition and crude oil density using the correlation chart, combined with the API chart established by Michael et al. (2013) for sample S_1 parameters. The final light hydrocarbon recovery factor obtained is 33% (Fig. 2). Conventional core samples experience varying degrees of volatilization and loss during processes such as pressure release and room temperature storage. Influenced by core storage conditions, laboratory testing and analytical techniques, as well as the adsorption and swelling effects of kerogen, there is a loss of light and heavy hydrocarbons in the S_1 parameter. These factors lead to measured values being significantly lower than the actual subsurface values (Fan et al. 2025), thus making it necessary to correct them. This study is consistent with the results of light hydrocarbon recovery using thermal simulation of hydrocarbon generation experiments by Wu et al. (2024).

3 Results and discussions

3.1 Geochemical characteristics

3.1.1 Thermal maturity

Thermal maturity is an essential for the evaluation of hydrocarbon source rocks (Thakur et al. 1984; Afonso et al. 1994; Tissot and Welte 1984). Vitrinite reflectance (R_o), is a reliable proxy of thermal maturity (Burnham 2019). The calculated R_o values range from 1.05% to 1.13% with an average of 1.09%, indicating that the thermal maturity is in the mature stage. The pyrolysis T_{max} and the potential index ($PI = (S_1/(S_1 + S_2))$ are also effective in evaluating the thermal maturity (Liu et al. 2024). Figure 3a shows that the T_{max} values range from 375 to 513 °C, with an average value of 425 °C. However, at a depth of 3700 m, the trend of the T_{max} values shows a significant reversal. Overall, with increased burial depth, the thermal maturity of organic matter increases. Comparison results of Figs. 3a and b show that when the PI values are high, the T_{max} values are suppressed, especially between depths of 3700 to 3730 m, and the T_{max} data is negatively correlated with the PI values. The results are inconsistent with the R_o analysis. Low T_{max} values are possibly due to crude oil contamination or the influence of micro-migration (Hu et al. 2021a; Hazra et al. 2021).

3.1.2 Organic matter types

Cross plot of T_{max} and hydrogen index (HI) can be used to characterize organic matter types (Huang et al. 1984; Wu et al. 2025b; Lis et al. 2005). Organic matter was categorized as Type I, Type II_1 with Type II_2, and Type III. Results show that T_{max} ranges from 375 to 513 °C, with an average value of 425 °C; HI ranges from 11 to 560 mg/g, with an average value of 175 mg/g. Type I samples have T_{max} ranging from 437 to 513 °C, with an average value of 469 °C; HI ranges from 17 to 560 mg/g, with an average value of 206 mg/g. Type II_1 samples have T_{max} temperatures ranging from

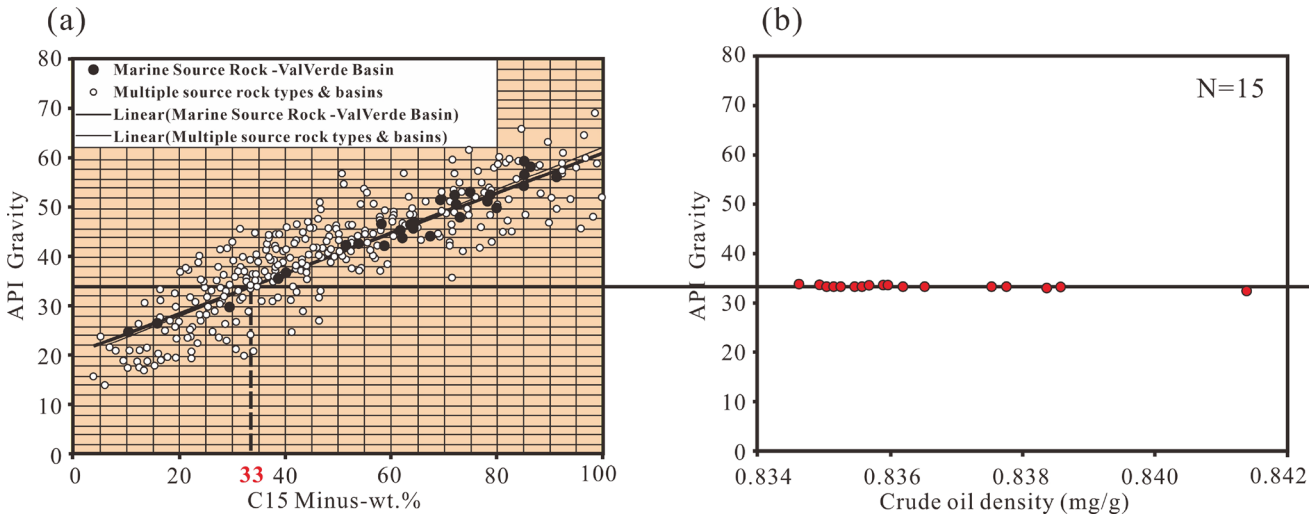

Fig. 2 **a** The plot of C_{15} Minus- and API Gravity was used for light hydrocarbon calibration (Michael et al. 2013); **b** Crude oil density versus API index of well Wen 318

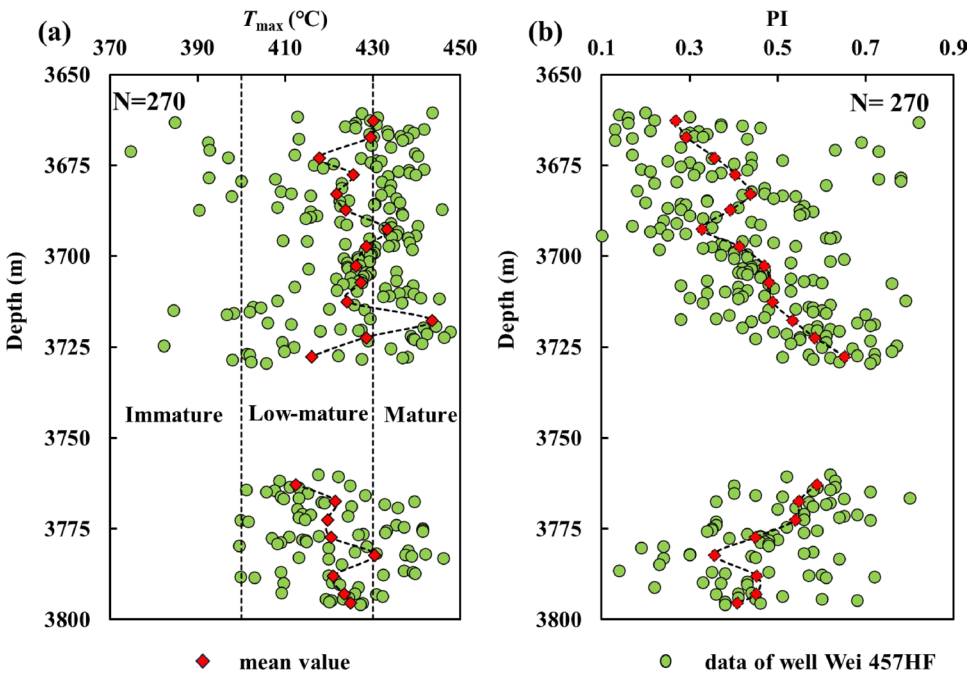

Fig. 3 T_{max} and PI vertical evolution of well Wei 457 HF **a** T_{max} versus Depth; **b** Production index (PI = $(S_1/(S_1+S_2))$ versus Depth

409 to 446 °C, with an average value of 434 °C; HI content ranges from 202 mg/g to 484 mg/g, with an average value of 317 mg/g. Type II_2 samples have T_{max} temperatures ranging from 375 to 460 °C, with an average value of 425 °C; HI content ranges from 29 mg/g to 275 mg/g, with an average value of 185 mg/g. Type III samples have T_{max} temperature ranges from 382 to 450 °C, with an average value of 417 °C; HI content ranges from 11 mg/g to 124 mg/g, with an average value of 83 mg/g. The HI-T_{max} plot indicates that the organic matter in the Wei 457HF shale is predominantly Type II_2 kerogen (50%), followed by Type II_1 (17%), Type III (31%) kerogen, and a minority of Type I (2%) (Fig. 4a). Hence, the organic matter Type in the Wei 457HF shale dominates in Type II_1 and Type II_2, indicating a strong oil-generating capability.

3.1.3 Organic matter abundance

Organic matter abundance is an important indicator for assessing the quality of hydrocarbon source rocks (Amer et al. 2023). TOC content and hydrocarbon generation

potential ($PG = S_1 + S_2$) are commonly used indicators for evaluating organic matter abundance (Tissot and Welte 1978; Peters 1986). Results show that the TOC content ranges from 0.06% to 3.6%, with an average of 0.86%. A total of 185 samples have values greater than 0.6%, with an average of 1.11%. As shown in Fig. 4b, TOC values of Type I kerogen range from 0.2% to 2.6%, with an average of 1.3%; PG values range from 0.07 to 16.4 mg/g, with an average of 6.5 mg/g. TOC values of Type II_1 kerogen range from 0.4% to 3.6%, with an average of 1.4%. PG ranges from 1.0 to 22.7 mg/g, with an average of 7.0 mg/g; 75.5% of the Type II_1 kerogen shale is considered fair to good source rocks. TOC values of Type II_2 range from 0.7% and 2.2%, with an average of 0.9%. PG values range from 0.2 to 14.6 mg/g, with an average of 3.6 mg/g. 73.9% of the Type II_2 kerogen shale samples are fair to good source rocks. TOC values of Type III kerogen range from 0.6% to 1.1%, with an average of 0.4%. PG values range from 0.02 to 3.1 mg/g, with an average of 0.8 mg/g. Most shale samples are ineffective source rocks (Fig. 4c), with few being of fair quality.

3.2 Variations in hydrocarbon generation potential and oil content

Zhou and Pang et al. used $((S_1 + S_2)/TOC*100)$ as the index of hydrocarbon generation potential (IHGP), which can be used to evaluate the hydrocarbon potential (Zhou and Pang 2002). The results showed that the IHGP values of different kerogen type shales in Wei 457HF shale were significantly different (Fig. 5c). The highest IHGP value was found in the lacustrine shale of Type II_1 kerogen, with a mean value of 496.0 mg/g (261.01–803.5 mg/g), followed by Type II_2, Type I, and Type III kerogen, with mean values of 375.7 mg/g (33.1–1103.6 mg/g), 272.3 mg/g (30.6–624.2 mg/g), and 190.1 mg/g (18.3–543.4 mg/g). Type III kerogen shales have limited hydrocarbon generation potential and should not be considered as targets for exploration and development, indicating differences in the hydrocarbon generation potential and organic matter types. Different types of kerogen exhibit distinct hydrocarbon generation capabilities and expulsion efficiencies for various hydrocarbon products. For Type III organic matter, due to the similarity in molecular structure, aromatics and non-hydrocarbons are difficult to expel from the source rock (Cai et al. 2007). Type I kerogen has the greatest hydrocarbon generation potential, followed

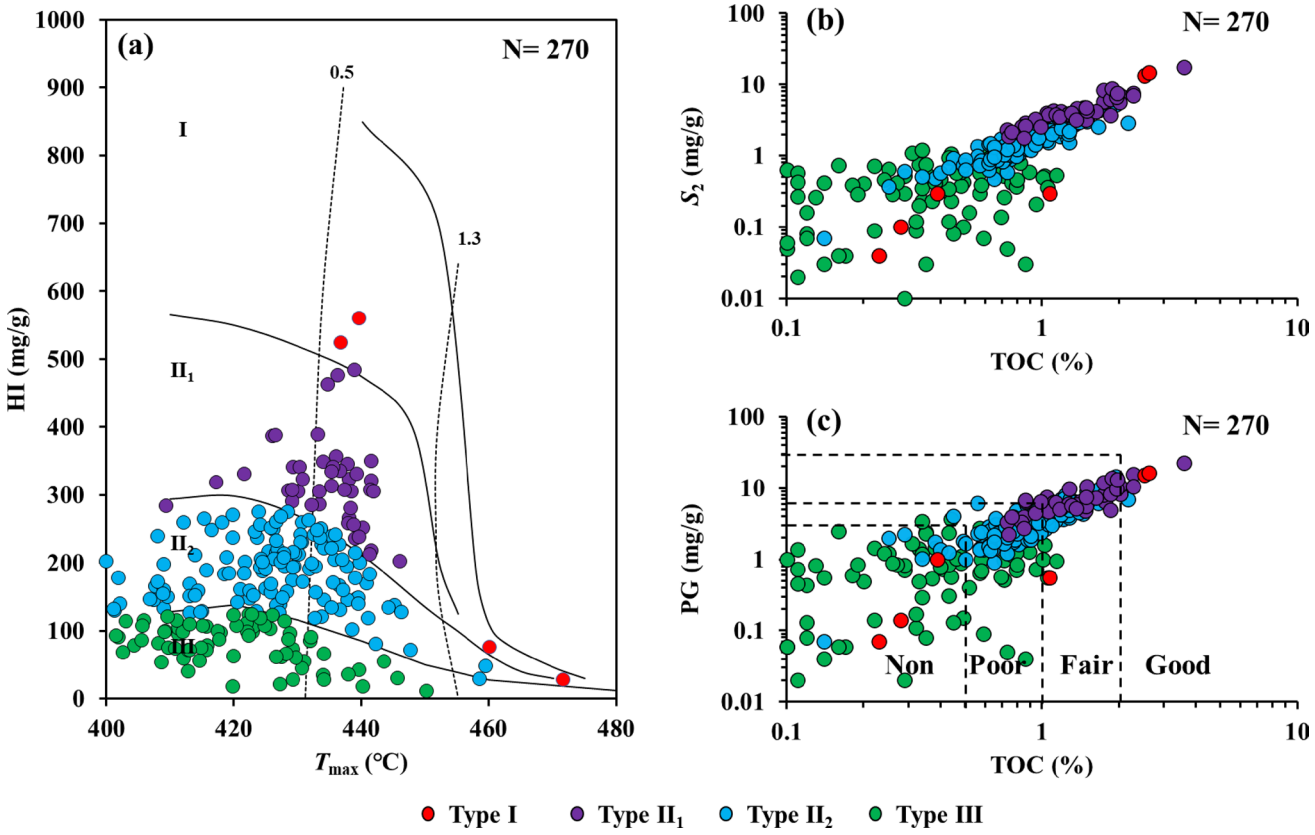

Fig. 4 Organic matter abundance, types, and maturity evaluation of the well Wei 457HF. **a** Hydrogen index (HI) versus T_{max}; **b** TOC versus pyrolysis S_2; **c** TOC versus petroleum generation potential (PG)

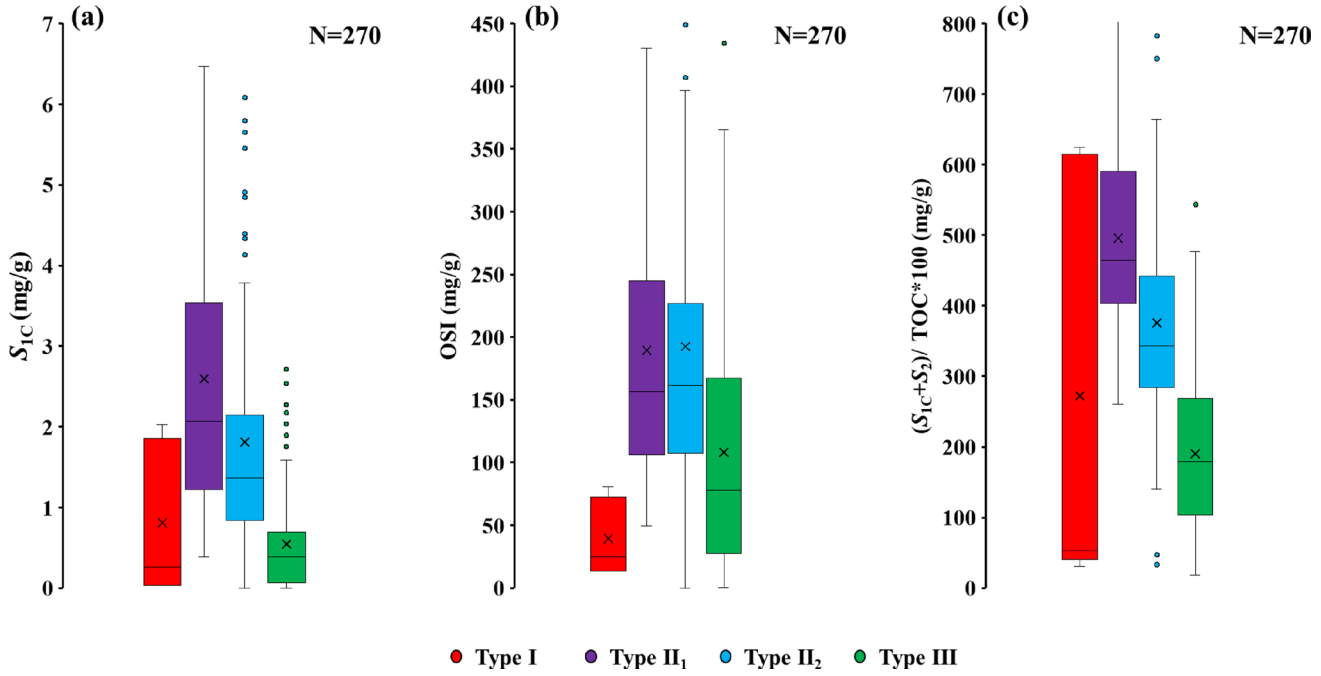

Fig. 5 Comparisons of the Shahejie Formation shales with different kerogen Types from the well Wei 457 HF. **a** Free hydrocarbon (S_{1C}); **b** Oil saturation index (OSI); **c** Hydrocarbon generation potential ($S_{1C}+S_2$/TOC)

by Type II_1 and Type II_2 kerogen, with Type III kerogen having the lowest potential.

The pyrolysis S_1 content is an important indicator for evaluating the oil content of shale oil (Romero-Sarmiento et al. 2019). The results show that lacustrine shales with Type II_1 kerogen have the highest S_{1C} values, followed by Type II_2, Type I, and Type III kerogen, with average values of 2.64 mg/g (ranging from 0.38 to 8.20 mg/g), 1.77 mg/g (ranging from 0.01 to 9.12 mg/g), 0.93 mg/g (ranging from 0.04 to 1.98 mg/g), and 0.54 mg/g (ranging from 0.01 to 2.65 mg/g). The oil saturation index (OSI = S_1/TOC*100) can be used to estimate the producible oil content of shale (Jarvie 2012). After light hydrocarbon calibration recovery, the OSI values of 270 shale samples from the E_2s in the Wei 457HF well vary with different types of kerogen. Lacustrine shales with Type II_1 kerogen have the highest OSI values, followed by Type II_2, Type III, and Type I kerogen, with average values of 189.4 mg/g (ranging from 49.3 to 496.1 mg/g), 187.5 mg/g (ranging from 0.1 to 862.3 mg/g), 108.2 mg/g (ranging from 0.2 to 434.4 mg/g), and 39.4 mg/g (ranging from 13.5 to 80.6 mg/g). Overall, the producible hydrocarbon content of lacustrine shale shows an increasing trend from Type I to Type II_1 kerogen, and a decreasing trend from Type II_1 to Type III kerogen (Figs. 5a, b). Due to the limited number of Type I kerogen samples, the results are not considered reliable and not discussed in detail.

3.3 Micro-migration identification and evaluation

In this study, the organic matter abundance of the Shahejie Formation. shale is relatively low, with 65% of the samples having a TOC content of less than 1%, and only 0.03% of the samples having a TOC content greater than 2%. Reducing conditions and increased water salinity may lead to low organic matter abundance in the E_2s shales of the DD and influence the group component of source rocks (Hu et al. 2018b). Moderate water salinity is conducive to the organic matter preservation and hydrocarbon transformation. However, extreme water salinity is not conducive to biological growth, leading to low organic matter abundance in source rocks (Rosenberg and Reznik 2021). Overall, the shale formation has poor hydrocarbon generation potential, not consistent with the organic matter abundance evaluation results mentioned earlier, indicating that results based on the average TOC values are not objective. The strong heterogeneity of HSS formations leads to with significant vertical variations. Thin layers or laminated argillaceous limestone may be more conducive to hydrocarbon expulsions. For instance, intercalated marlstone layers of Ordovician shale formations in the North American and Australian platforms do not have high organic matter abundance, and are considered the main oil-generating intervals (Johnson et al. 2022). In the DD, the OSI values of the shales tend to decrease with increasing TOC. Shales with an OSI greater than 100 mg/g are primarily shales with relatively low

organic matter abundance (TOC < 1%). For samples with TOC greater than 1%, their OSI values are generally lower (Fig. 6a). These indicate that the organic-rich shales generate oil and gas that is migrated to the lower organic matter abundance laminated shales. Shales with lower TOC content exhibit higher S_{1C} values, proving the occurrence of shale oil micro-migration (Fig. 6b). The PI versus TOC and T_{max} versus TOC also indicates that the shale oil enrichment is influenced by micro-migration, resulting in the micro-migration from organic-rich type I shales to organic-poor Type II_2 or Type III shales. This exhibits a clear positive anomaly in OSI values, a positive anomaly in PI, and a negative anomaly in T_{max}. The lower the TOC, the more pronounced the anomaly (Figs. 6c, d). After the oil micro-migration geochemical data shows a decrease in their own S_{1C} values and results in lower OSI value. When the oil from relatively organic-rich Type I and II_1 shales satisfies the adsorption capacity of the shale itself, it begins to expel hydrocarbons towards adjacent shales with better reservoir capabilities that have lower organic matter content. Overall, from the relatively higher TOC Type I and II_1 shales to the relatively lower TOC Type II_2 and Type III shales, there is a trend of increasing OSI and PI, and decreasing T_{max} (Figs. 6e, f). This demonstrates the characteristic of oil generated from relatively organic-rich shales being internally migrated to relatively organic-poor shales. The enrichment of crude oil within the shale (including migrated crude oil and oil that is locally retained and enriched) results in shale samples having higher OSI values, higher PI values, and lower T_{max} values (Liu et al. 2024).

Jiang et al. proposed a method for identifying the source of residual hydrocarbons through a PI-T_{max} plot, suggesting that when T_{max} is between 430 and 460 °C and PI is between 0.05 and 0.4, the shale is in the hydrocarbon generation phase, generating its own hydrocarbons. When T_{max} is too low or PI is too high, it indicates the exhibit hydrocarbon charging phenomenon from external sources (Hang 2015). Based on this plot (Fig. 7a), the residual hydrocarbon source of 270 shale samples from the Wei 457HF well was

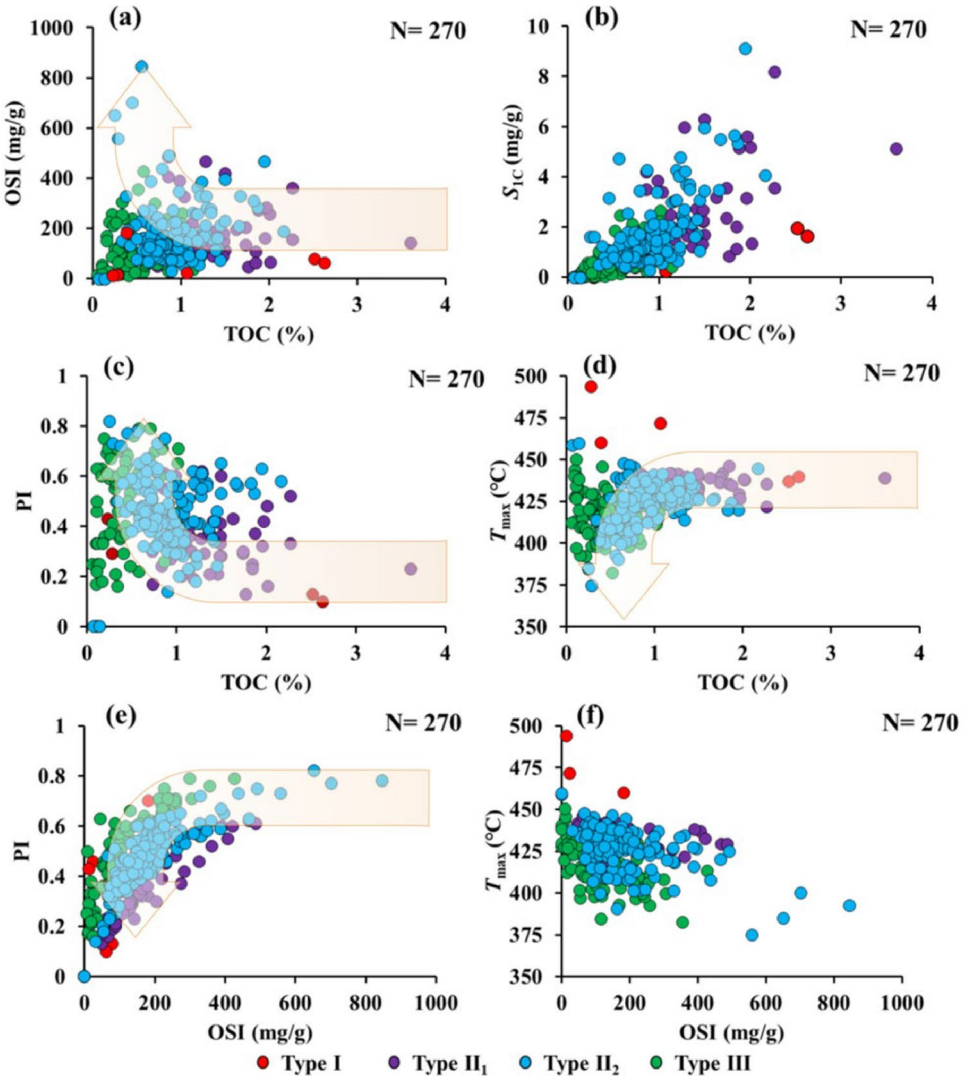

Fig. 6 Geochemical data anomalies of the well Wei 457 HF suggest significant oil micro-migration. **a** OSI versus TOC; **b** S_{1C} versus TOC; **c** PI versus TOC; **d** T_{max} versus TOC; **e** PI versus OSI; **f** T_{max} versus PI

identified, and the results indicate that a large number of samples exhibit exhibit hydrocarbon charging phenomenon from external sources. Additionally, samples with evidence of hydrocarbon charging have higher OSI values. Chen et al. proposed a hydrocarbon generation kinetics diagram using the ratio $S_2/(S_{1C}+S_2)$ versus T_{max} to determine the extent of influence from the exhibit hydrocarbon charging phenomenon of external migrated hydrocarbons on the samples (Bonnaud et al. 2023). When T_{max} is less than 430 °C, the $S_2/(S_{1C}+S_2)$ ratio is relatively low, indicating a higher content of free hydrocarbons. However, at this point, the hydrocarbon source rock is in a stage where it has not generated a large amount of hydrocarbons. As T_{max} increases, the amount of generated hydrocarbons increases, and the $S_2/(S_{1C}+S_2)$ ratio decreases. The normal evolutionary trend of hydrocarbon generation kinetics is as shown in the diagram (Fig. 7b), but the evolutionary pattern in the $S_2/(S_{1C}+S_2)$-T_{max} plot deviates from the normal trend. Therefore, it is determined that there is a micro-migration of hydrocarbons in the source rock. As indicated in Figs. 7a,b, Type I and II_1 shale samples have strong hydrocarbon generation capabilities, and the generated oil is primarily retained in place. Type II_2 and Type III shale samples have poor hydrocarbon generation capabilities and high OSI, indicating that they are mainly enriched through micro-migration.

This study employed the hydrocarbon expulsion potential method proposed by Hu et al., to conduct a quantitative evaluation of the amount of micro-migration hydrocarbons in the E_2s shales of the DD (Hu et al. 2024b). The results of micro-migration hydrocarbon calculations for 270 shale samples showed that the distribution of ΔQ values of the shales of the E_2s was in the range of − 846 to 993 mg/g, with an average value of − 120 mg/g. Among the 270 samples, 242 samples exhibit hydrocarbon expulsion charging phenomenon (ΔQ < 0), accounting for 90% of the samples, and the amount of charging ranges from 0 to 846 mg/g, with an average value of 157 mg/g. 28 samples exhibit hydrocarbon expulsion charging phenomenon (Δ Q > 0), accounting for 10% of the samples, and the amount of expelled hydrocarbon ranges from 0 to 993 mg/g, with an average value of 94 mg/g, indicating that most of the shale samples exhibit hydrocarbon expulsion phenomenon. In Type I samples, 2 samples exhibit the hydrocarbon charging phenomenon (ΔQ < 0), accounting for 40%, ranging from − 23 to − 14 mg/g, with an average value of − 18 mg/g; 3 samples experienced hydrocarbon expulsion (ΔQ > 0), accounting for 60%, ranging from 112 to 993 mg/g, with an average value of 604 mg/g. In Type II_1 samples, 40 samples exhibit the hydrocarbon charging phenomenon (ΔQ < 0), accounting for approximately 89%, ranging from − 487 to − 18 mg/g, with an average value of − 172 mg/g; 5 samples experienced hydrocarbon acceptance (ΔQ > 0), accounting for approximately 11%, ranging from 10 to 77 mg/g, with an average value of 38 mg/g. In Type II_2 samples, 127 samples exhibit the hydrocarbon charging phenomenon (ΔQ < 0), accounting for approximately 93%, ranging from − 846 to − 9 mg/g, with an average value of − 177 mg/g; 9 samples experienced hydrocarbon acceptance (ΔQ > 0), accounting for approximately 7%, ranging from 8 to 159 mg/g, with an average value of 45 mg/g. In Type III samples, 73 samples exhibit the hydrocarbon charging phenomenon (ΔQ < 0), accounting for approximately 88%, ranging from − 428 to 0 mg/g, with an average value of − 117 mg/g; 11 samples experienced hydrocarbon acceptance (ΔQ > 0), accounting for approximately 12%, ranging from 0 to 63 mg/g, with an average value of 20 mg/g (Figs. 8a–d). The results show that Type I kerogen is primarily dominated by hydrocarbon expulsion; Type II_1 kerogen has both expulsion and hydrocarbon charging; Type II_2 and Type III are mainly characterized by the exhibit hydrocarbon charging, with Type II_2 having the highest amount of micro-migration hydrocarbons (Fig. 8e). The differences in the amount of micro-migration hydrocarbons ΔQ among different types of kerogen indicate that different types of kerogen have varying hydrocarbon generation and expulsion efficiencies.

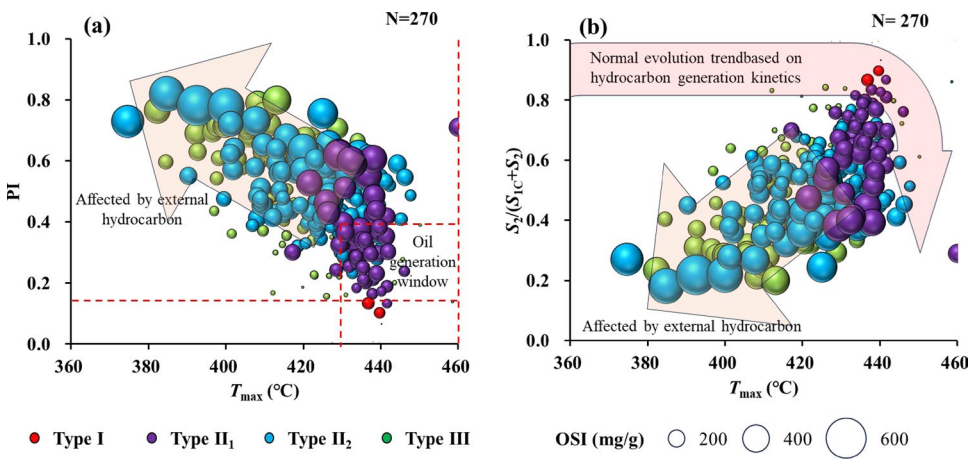

Fig. 7 Shale micro-migration hydrocarbon identification. **a** PI versus T_{max}; **b** $S_2/(S_{1C}+S_2)$ versus T_{max}

Kerogen classification is primarily divided into sapropelic components, followed by chitin, vitrinite, and inertinite components. The sapropelic components mainly originate from lower planktonic organisms that are rich in proteins and lipid compounds, with sub-fractions including algal bodies and amorphous substances; the chitin's precursors are mostly chitinous tissues from terrestrial or aquatic higher plants; the vitrinite's precursors come from the woody parts of higher plants; the inertinite components also originate from higher plants, being formed from the carbonization of the woody parts of higher plants (Wu et al. 2025b). The type of kerogen mainly depends on the relative proportions of lipid-rich algal bodies, amorphous substances, spores, and other components of the sapropelic group, including wood, fibers, and vitrinite, in the kerogen composition (Huang et al. 1984). Different types of organic matter have different hydrocarbon generation potentials and produce different types of products. The thresholds for hydrocarbon generation and the hydrocarbon generation processes also differ to some extent. This is primarily related to the chemical composition and structure of the organic matter (Rosenberg and Reznik 2021). The fundamental reason for the different hydrocarbon generation capabilities of different types of kerogen is the variation in the hydrocarbon parent material, and the depositional environment influences the source supply of sedimentary organic matter (Gama and Schwark 2023). According to Tissot's model for organic matter hydrocarbon generation, from sapropelic (Type I) to humic (Type III) kerogen, the oil-generating ability of the organic matter decreases progressively. Therefore, deep lake and semi-deep lake sedimentary environments are necessary conditions for the generation and accumulation of shale oil. Based on the results of hydrocarbon generation simulation experiments on terrestrial organic-rich mud shales, the oil generation rate of

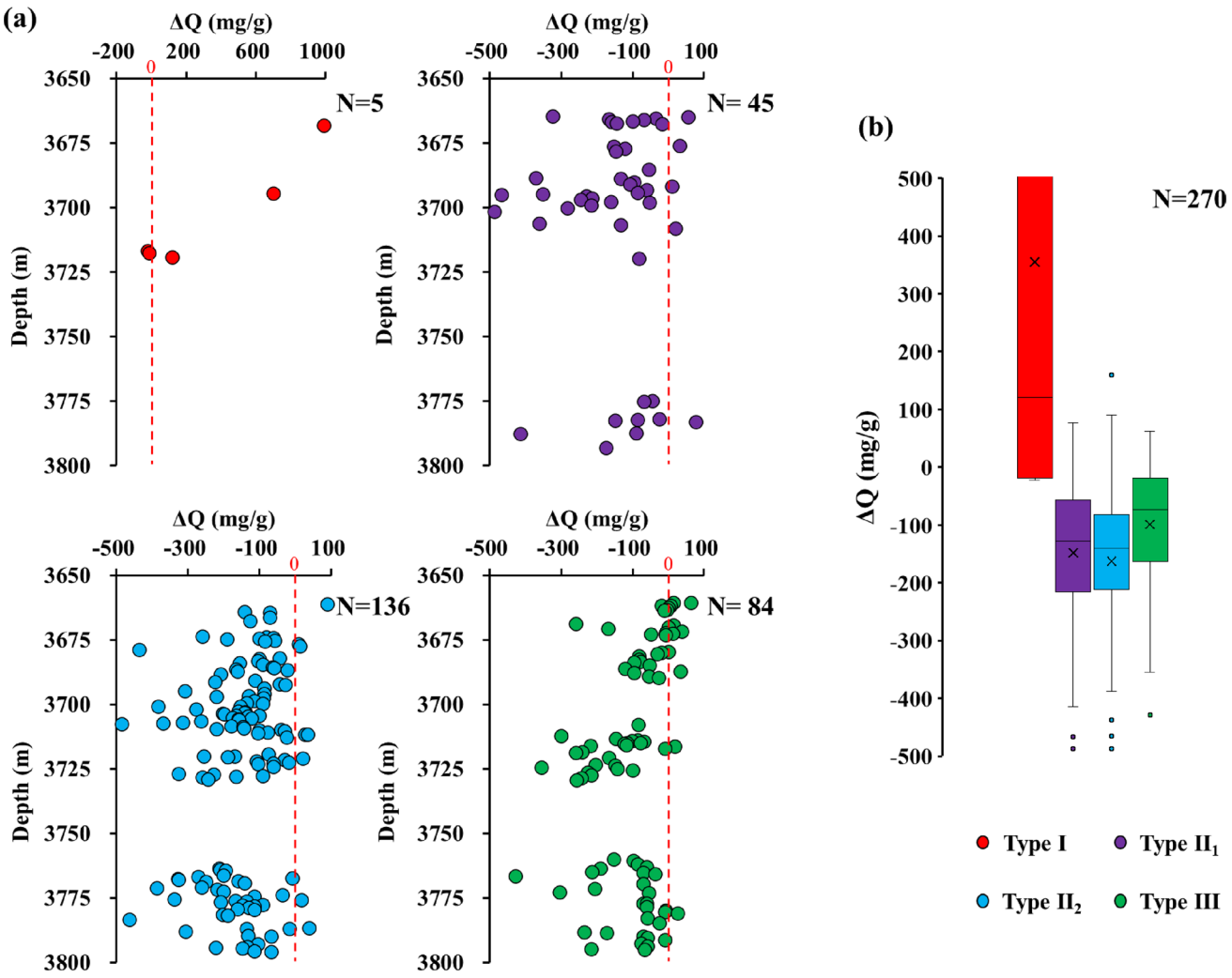

Fig. 8 Micro-migration hydrocarbons vertical evolution with different kerogen types of the well wei 457HF. **a** ΔQ versus depths; **b** Micro-migration hydrocarbons comparison of different kerogen types

Type I kerogen can be 10 times or more than that of Type III kerogen, and the oil generation rates of Type II_1 and Type II_2 kerogen can be 2 to 7 times that of Type III kerogen (Zhang et al. 2012; Hu et al. 2021b). Different sedimentary environments lead to variations in the hydrocarbon parent material of kerogen. Different types of kerogen originate from various parts of algae and higher plants. From the perspective of hydrocarbon generation capability, the different types of kerogen result in varying oil-generating abilities. The higher the proportion of sapropelic components, the stronger the oil-generating capability.

Fluorescent cast thin sections reveal the presence of microcracks (Figs. 9a-c). This indicates that micro-migration is more likely to occur in shales with good pore connectivity or those with structural fractures or micro-migration caused by oil/hydrocarbon generated overpressure (Safaei-Farouji et al. 2023). Moreover, the fluorescence of the Type II_1 samples is relatively strong, while the fluorescence within the microcracks is weaker. This suggests that part of the generated shale oil is retained and has undergone micro-migration. However, Type II_2 and Type III shale layers exhibit no fluorescence overall, with fluorescent reactions only occurring within the microcracks, Due to insufficient data from the Wei 457HF well, three laser confocal scanning samples of different kerogen types from a nearby well location were selected. As shown in Figs. 10a–f, Type II_1 samples are essentially filled with blue heavy oil and green light oil, while Type II_2 and Type III samples are predominantly filled with green light hydrocarbons, distributed along the laminations. This confirms the phenomenon of micro-migration, and it is inferred that Type II_1 shales generate hydrocarbons, and the shale oil undergoes micro-migration through microcracks into the Type II_2 and Type III shale.

In terms of migration pathways and preservation conditions, during the hydrocarbon generation and evolution of organic matter, it is beneficial to improve the reservoir properties of shale. The porosity increases with the thermal decomposition process of kerogen and the generation of

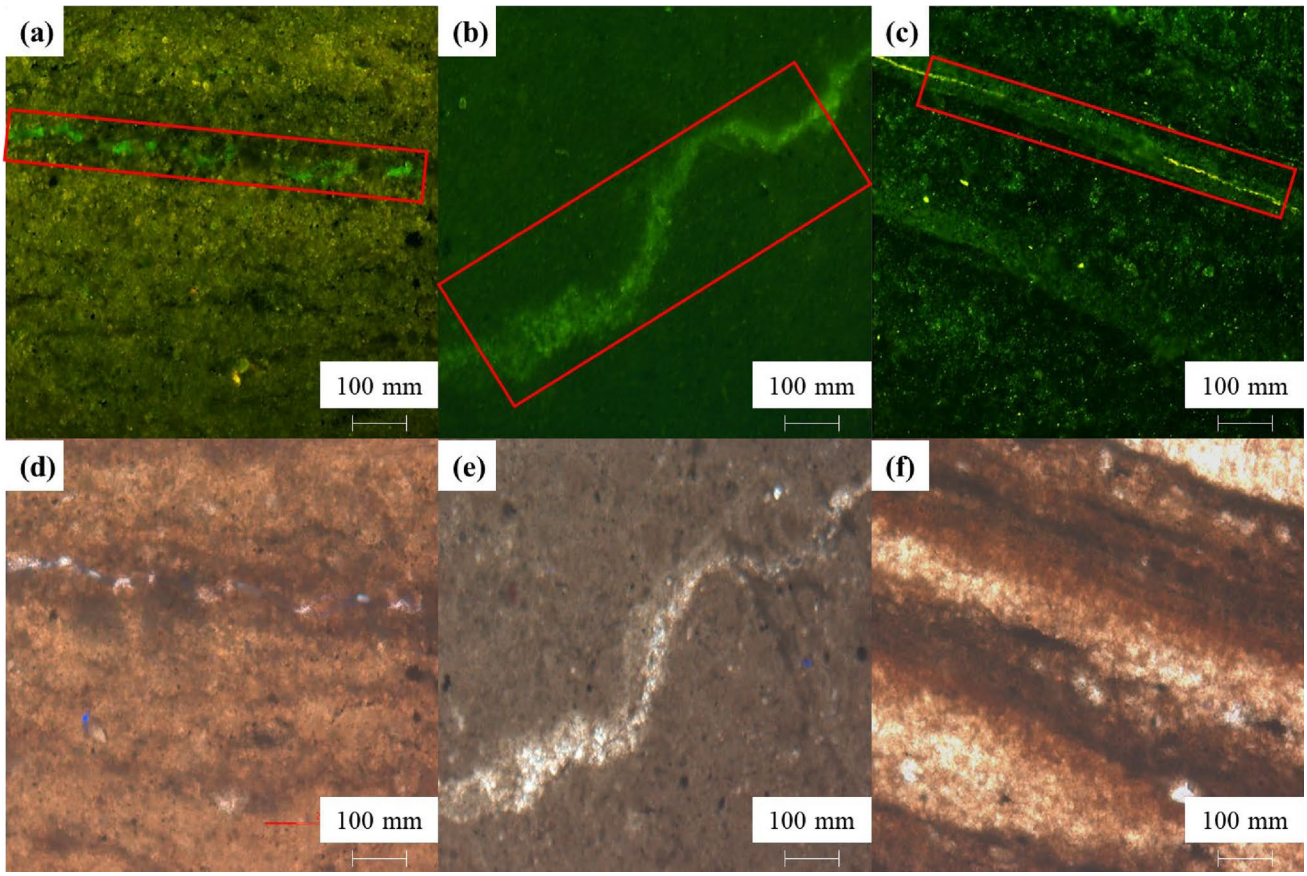

Fig. 9 Thin section fluorescence map of different kerogen in shale of E_2s. **a** 3694.82 m, Type II_1 kerogen, mudstone fluoresces yellowish-green with medium luminous intensity, microcracks fluoresce light blue with weak luminous intensity; **b** 3688.25 m, Type II_2 kerogen, mud crystal chert does not fluoresce as a whole, the leucocrystalline calcite in the microcrack fluoresces yellowish green with weak luminous intensity; **c** 3712.19 m, Type III kerogen, mud stripe fluoresces yellowish-green with weak luminous intensity, carbonate stripe does not fluoresce; **d** 3694.82 m, Type II_1 kerogen, of single-polarized light; **e** 3688.25 m, Type II_2 kerogen, of single-polarized light; **f** 3712.19 m, Type III kerogen, of single-polarized light

hydrocarbons (Salter et al. 2023). Different types of kerogen have a certain impact on the development of micro-pores in shale. As kerogen transitions from mixed types to sapropelic types, both the specific surface area and the pore volume of the mud shale decrease (Ariskina et al. 2024). Previous studies have shown that, under similar conditions, the specific surface area and pore volume of micro-pores in shales containing Type II kerogen are greater than those in shales containing Type I kerogen. The reason may be that as kerogen transitions from Type I to Type II_1, and from Type II_1 to Type II_2, the proportion of sapropelic components decreases while the content of other components increases. The sapropelic components are mainly formed from lower organisms such as bacteria and algae and their degradation products, whereas Type II kerogen originates from higher plankton. The internal structure of higher planktonic organisms is larger and more complex compared to that of lower bacteria and algae. Type II kerogen formed from higher planktonic organisms contains polycyclic aromatic hydrocarbons and heteroatom functional groups (Baudin et al. 2024). Therefore, the micro-pores of Type II kerogen are typically larger than those of Type I, which leads to an increase in the micro-pore space of the shale. This also affects the specific surface area and pore volume of the shale (Patel et al. 2024). During the diagenesis of clastic reservoirs, the thermal evolution of organic matter in source rocks can release a large amount of organic acids, which strongly dissolve aluminosilicate and carbonate minerals, thereby forming significant secondary porosity. In the thermal evolution stages of different types of organic matter, the amount of organic acids generated varies. As seen in Table 1, Type III kerogen produces more acids than Type II_2, which in turn produces more than Type II_1. The more organic acids released, the more aluminosilicate and carbonate minerals are dissolved, leading to the formation of more secondary porosity. Therefore, it is speculated that the pore conditions in Type III kerogen strata might be relatively better. Type I also has a good acid production, which may be due to the strong hydrocarbon generation capability leading to a higher total amount of organic acids produced. The greater the amount of organic acids generated, the better the secondary porosity conditions, providing shale oil with good storage spaces and migration pathways,

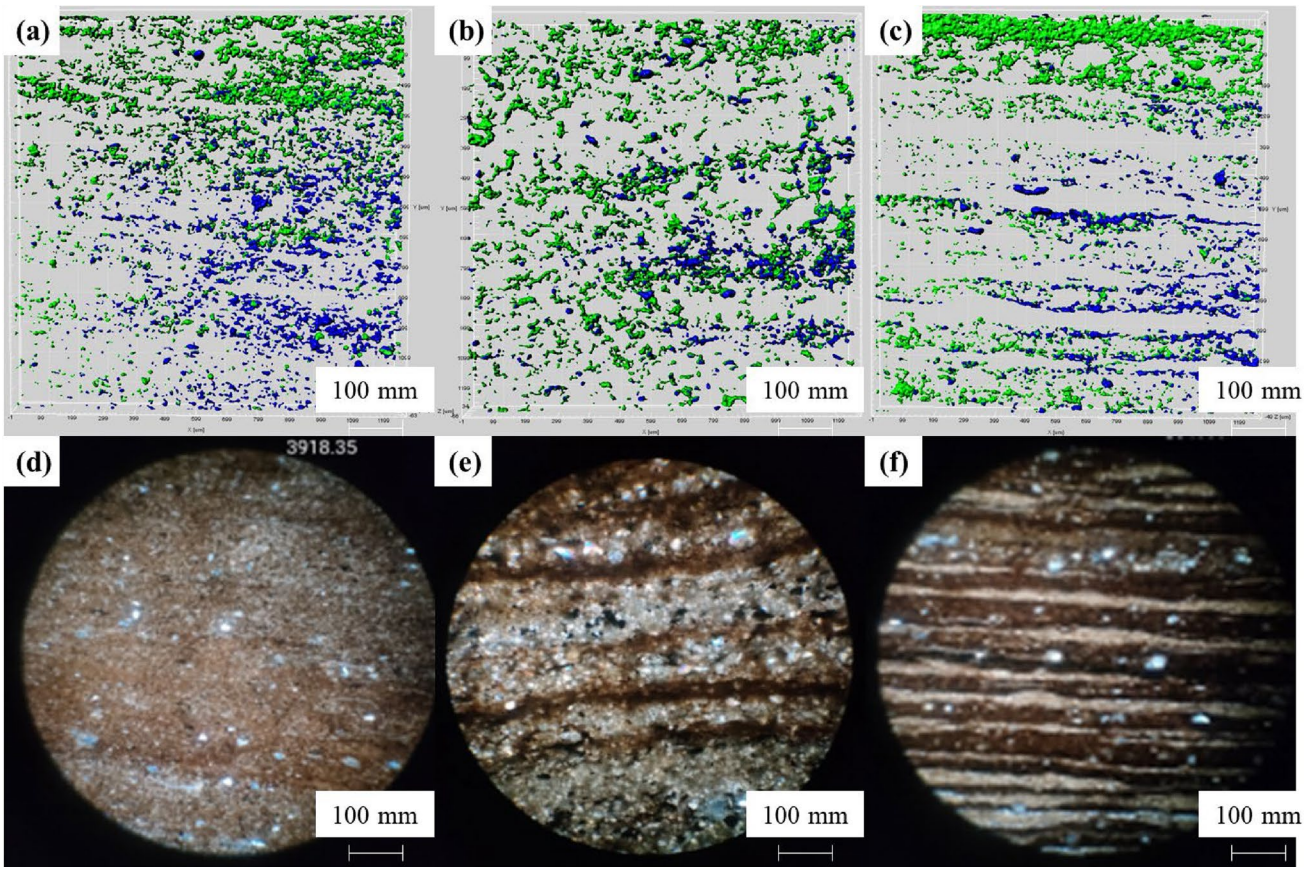

Fig. 10 Laser confocal and Microscopic observation of different kerogen in shales of the E_{2S}. **a** 3830.1 m, Type II_1 kerogen, laminated felsic gray shale; **b** 3832.2 m, Type II_2 kerogen, laminated felsic shale; **c** 3850.83 m, Type III kerogen, laminated felsic shale. **d** 3830.1 m, Type II1 kerogen, laminated felsic gray shale; **e** 3832.2 m, Type II_2 kerogen, laminated felsic shale; **f** 3850.83 m, Type III kerogen, laminated felsic shale

hence the higher amount of micro-migration hydrocarbons in Type II_2 and Type III kerogen. The overpressuring from hydrocarbon generation in Type I and Type II_1 kerogen, leading to the formation of fractures, also serves as a pathway for the micro-migration of shale oil (Zhang et al. 2009). However, the shale oil in Type I and Type II_1 kerogen shales has mostly undergone micro-migration, leaving little residual oil. Type II_2 and Type III kerogen shales have poor hydrocarbon generation capabilities. Nevertheless, they have good preservation conditions and superior permeability, which are more conducive to the enrichment of shale oil. Therefore, in terms of shale oil exploration, focus can be directed more towards the low organic matter abundance Type II_2 and Type III shale.

3.4 Shale oil resource evaluation and sweet spot prediction

Based on the shale oil resource classification criteria proposed by Hu et al. shale oil resources in DD shale (Fig. 11) were classified into enriched resources ($S_{1C} > 3.5$ mg/g and OSI > 100 mg/g), moderately enriched resources (0.5 mg/g < S_{1C} < 3.5 mg/g and OSI > 100 mg/g), less efficient resources (0.5 mg/g < S_{1C} < 3.5 mg/g and OSI < 100 mg/g) and invalid resources ($S_{1C} < 0.5$ mg/g and OSI < 100 mg/g) (Hu et al. 2018a). After dividing into four different categories of resource volumes, Fig. 12 shows that the amount of micro-migration hydrocarbons varies in different areas. The highest amount of micro-migration hydrocarbons is found in enriched resources, followed by moderately enriched resources, less efficient resources, and invalid resources. In the DD, E_2s, high-quality and average resources are predominantly composed of Type II_1 and Type II_2 kerogen. It is this part of the enriched and moderately enriched resources that possess commercial production capacity.

Due to differences in sediment sources, depositional environments, and mineral (including organic matter) compositions, the critical values for the "trichotomy" of oil content in different source rock layers vary (see Table 2) (Li 2021).

Table 1 TOC, kerogen types, Ro, and total acid yield of different shale samples in the Dongying Depression (Lu et al. 2012)

Hydrocarbon source rock place of origin	Sample number	TOC (wt%)	Types	R_o	Total acid yield (mg/g)
Dongying Depression Chun 11 Well	5	3.5	I	0.32	10.71–26.42
Dongying Depression Cao 13–15 Well	3	2.29	II_1	0.32	1.95–14.19
Dongying Depression Ying 10 Well	3	1.19	II_2	0.48	4.09–27.31
Dongying Depression Mian 4-5-16 Well	1	1.32	III	0.36	54.07

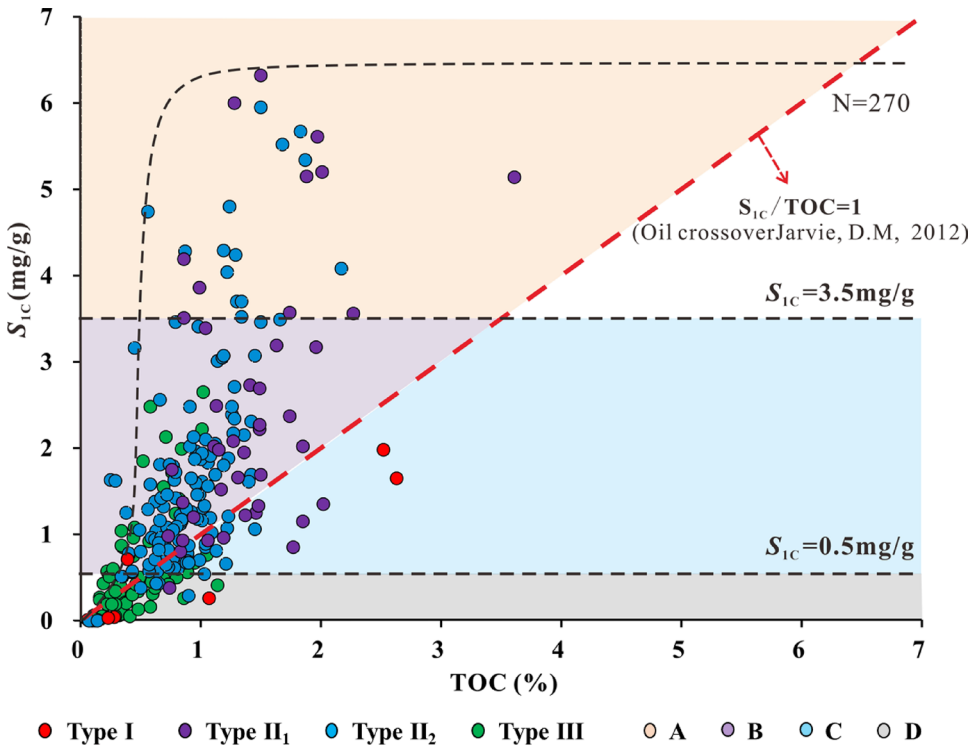

Fig. 11 Shale oil evaluation criteria of HSS shales in the DD. (Note: A Enriched resources ($S_{1C} > 3.5$ mg/g and OSI > 100 mg/g); B Moderately enriched resources (0.5 mg/g < S_{1C} < 3.5 mg/g and OSI < 100 mg/g); C Less efficient resources (0.5 mg/g < S_{1C} < 3.5 mg/g and OSI < 100 mg/g); D Invalid resources ($S_{1C} < 0.5$ mg/g and OSI < 100 mg/g)

The S_1 critical value of the E_2s in the DD is lower than the grading evaluation standards established by other scholars. Compared to the main shale basins in North America, Chinese shale basins are characterized mainly by the difference between marine and terrestrial shale oil. The relationship between oil content and TOC in the Qingshankou Formation of the southern Songliao Basin, the Lucaogou Formation of the Jimusaer Depression, and the Xingouzui Formation of the Jianghan Basin also reflects a "trichotomy," and all are higher than that of the E_2s in the DD. The mineral composition of the shale in the Qingshankou Formation of the Songliao Basin is predominantly clay minerals, which have a strong adsorption capacity, leading to higher TOC values. The Lucaogou Formation in the Jimusaer Depression and the Qingshankou Formation in the southern Songliao Basin are mainly characterized by Type II_1 kerogen, whereas the E_2s in the DD is primarily composed of Type II_2 kerogen, indicating different sources of hydrocarbon parent material. The lithology of the Xingouzui Formation in the Jianghan Basin is mainly argillaceous dolomite, while the lithology of the E_2s in the DD is primarily mud shale. Due to regional differences, varying depositional environments, different geological strata, and the distinct geological and tectonic processes experienced, there are differences in the critical points. Although we analyzed the results of the DD in comparison with other typical depressions, some problems still

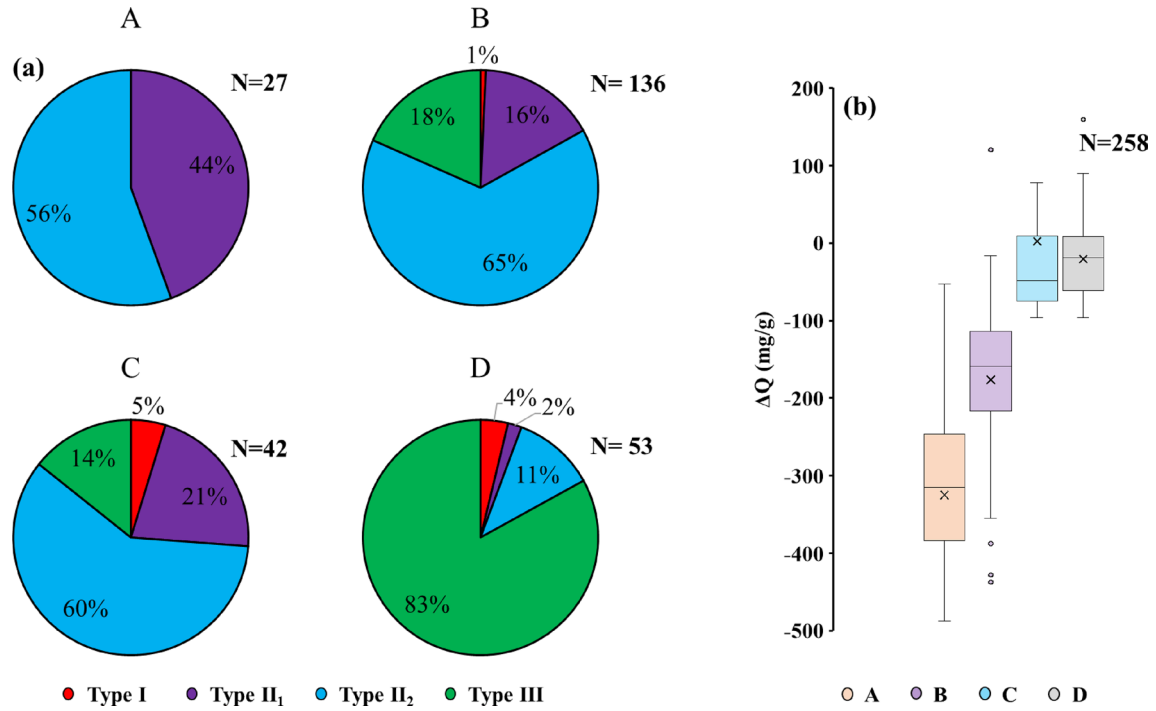

Fig. 12 **a** HSS shale oil resources percentage of four kerogen types; **b** Micro-migration hydrocarbon comparisons of different shale oil resources types

Table 2 S_1 boundaries in different basins and depressions (Hu et al. 2018a; Li et al. 2015b; Li 2021)

Basin (Depression)	Hydrocarbon source rock	TOC (wt%)	S_1 boundary 1 (mg/g)	S_1 boundary 2 (mg/g)
Southern Songliao Basin	Nenjiang Formation	0–7.4	0.5	1.8
Gulong Sag Songliao Basin	Qingshankou Formation	0–4.5	0.8	3.8
Jianghan Basin	Xingouzu Formation	0–8.0	1	4
Junggar Basin	Lucaogou Formation	0–19	1	4
Williston Basin	Bakken Formation	0–28	2	6
Denver Basin	Niobrara Formation	0–29	1.2	3.5
Permian Basin	Wolfcamp Formation	0–6.5	0.6	2.5
Dongpu Depression	Shahejie Formation	0–3.6	0.5	3.5

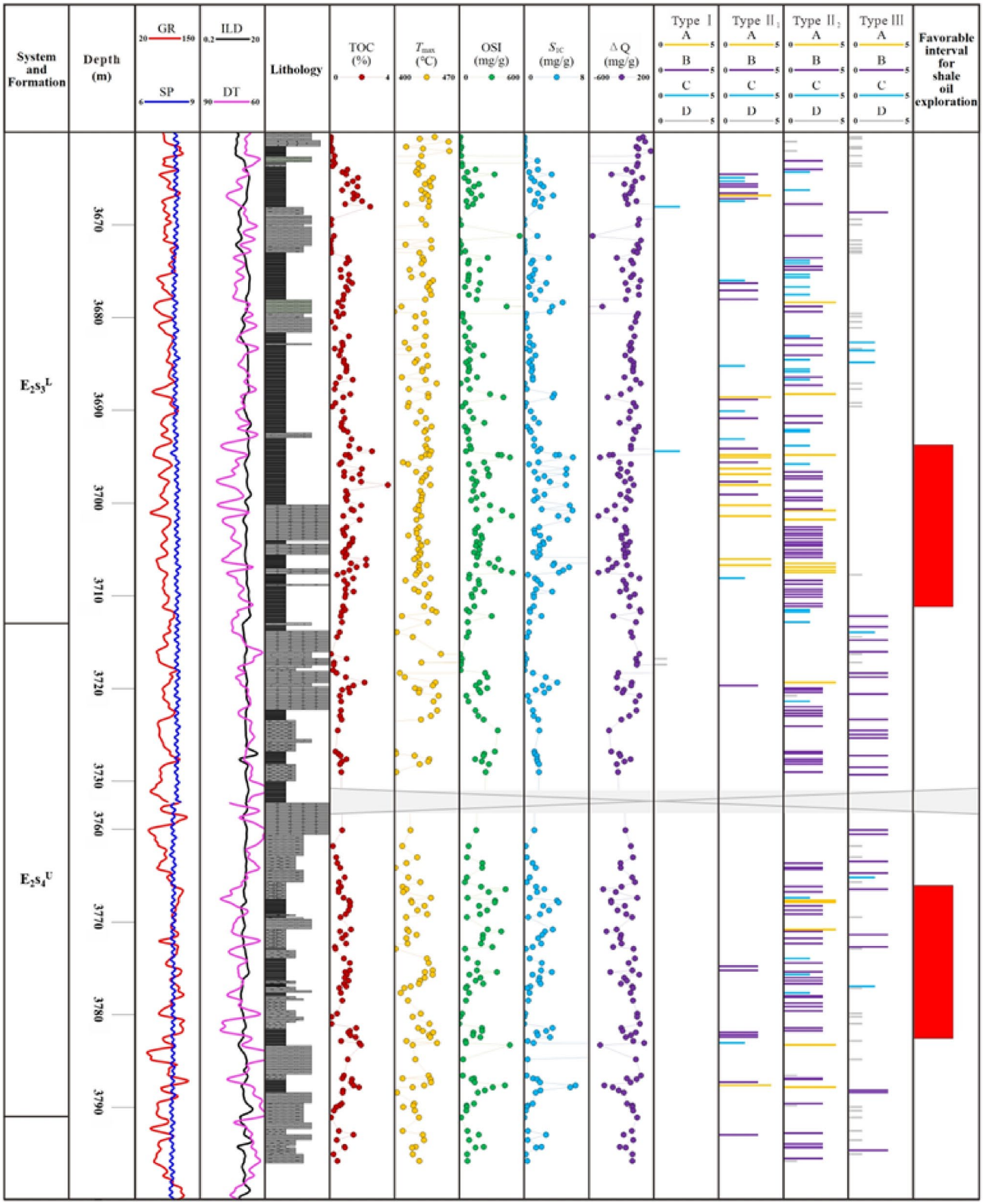

Fig. 13 The profile of the Wei 457HF well, showing the variation in shale oil potential of $E_2s_3^L$ and $E_2s_4^U$, DD

need to be clarified. First, we acknowledge that the current sample set is concentrated in a specific geological area. Systematic and random biases may exist during the sampling process, which might not be sufficient to represent broader geological conditions. Meanwhile, the sampling depth, location selection, and sample preservation processes may also introduce biases. These biases may have certain impacts on the research results. Secondly, instrument precision limitations and experimental condition variations have potential impacts on the results. In particular, there are differences between simulated experimental conditions and actual geological conditions. These differences may affect the practical application value of the data. At the same time, the hydrocarbon micro-migration model has certain limitations. For example, when preservation conditions are good, the identified amount of hydrocarbon micro-migration is relatively small. In this case, it is difficult to distinguish between the hydrocarbon receiving and the hydrocarbon expulsion units. When T_{max} is too small or too large, the determined values are also inaccurate. If T_{max} is calibrated, the results may be more accurate and effective. Finally, we acknowledge that the current classification system is primarily based on shale samples from DD, which may not be fully applicable to shales with significantly different mineral composition, type of organic matter, or maturity. We establish oiliness gradation of hybrid sedimentary shale with low-moderate organic matter content. However, it still has important significance for the oiliness gradation of hybrid sedimentary shale with low-moderate organic matter content in continental lacustrine basins worldwide. There are many influencing factors, and such simple comparative results should be used only as a reference.

Using the established grading evaluation criteria, the shale oil dessert layer section of shale in Wei 457HF area is divided for different kerogen types. The results show that at depth intervals of 3692–3710 m in $E_2s_3^L$ and 3765–3776 m in $E_2s_4^U$ of Wei 457HF wells, the resources are mainly enriched and moderately enriched (Fig. 13). This layer section is favorable for shale oil exploration; other depth intervals are mainly invalid resources with low exploration potential. Therefore, it is considered that the most favorable exploration interval for shale in Wei 457HF well should be $E_2s_3^L$, followed by $E_2s_4^U$. In this study, for the HSS with low organic matter abundance, a grading evaluation standard based on oil content combined with micro-migration hydrocarbon volume was finally established, which provides an important guidance for further lake-phase shale oil exploration in other regions of the world.

4 Conclusions

This study selected 270 continuous HSS cores from Wei 457HF well (Shahejie formation, Dongpu Depression, Bohai Bay Basin) and employed TOC analysis, pyrolysis analysis, fluorescence microscope observation, laser confocal scanning and hydrocarbon expulsion potential method to establish oil grading criteria for HSS with low-moderate organic matter abundance.

(1) The results indicate that the shale is overall at the mature stage, dominated by Type II_1 and Type II_2 kerogen, and is classified as fair to good hydrocarbon source rocks of the E_2s in the DD. And the different kerogen types had different micro-migration rates, in which the micro-migration of kerogen in Type II_2 was the highest.
(2) Established oiliness gradation of hybrid sedimentary shale with low-moderate organic matter content. This study classifies into enriched resources ($S_{1C} > 3.5$ mg/g and OSI > 100 mg/g), moderately enriched resources (0.5 mg/g < S_{1C} < 3.5 mg/g and OSI > 100 mg/g), less efficient resources (0.5 mg/g < S_{1C} < 3.5 mg/g and OSI < 100 mg/g) and invalid resources ($S_{1C} < 0.5$ mg/g and OSI < 100 mg/g), accounting for 11%, 53%, 16% and 21%, respectively.
(3) High-quality and general resources are mainly shale layers dominated by Type II_1 and Type II_2 kerogen and with large amounts of externally transported hydrocarbons, so the $E_2s_3^L$ in the DD, followed by $E_2s_4^U$, is the sweet spot for further shale oil exploration.

Supplementary Information The online version contains supplementary material available at https://doi.org/10.1007/s40789-025-00805-1.

Acknowledgements This study was financially supported by the National Natural Science Foundation of China (U24B6002, 42202133, U22B6004), CNPC Innovation Fund (2022DQ02-0106), Key Laboratory of Tectonics and Petroleum Resources of the Ministry of Education (TPR-2023-05), major science and technology projects of CNPC during the "14th five-year plan" (2021DJ0101), National Natural Science Foundation of China (41872148, 42072174, 42130803), Strategic Cooperation Technology Projects of the CNPC and CUPB (ZLZX2020-01-05), Sinopec Zhongyuan Oilfield and CUPB Cooperation Project (31300027-23-ZC0613-0013), AAPG Foundation Grants-in-Aid Program (22272306).

References

Afonso JC, Schmal M, Cardoso JN (1994) Hydrocarbon distribution in the irati shale oil. Fuel 73:363–366

Altawati F, Emadi H, Pathak S (2021) Improving oil recovery of eagle ford shale samples using cryogenic and cyclic gas injection methods—an experimental study. Fuel 302:121170

Amer MW, Aljariri Alhesan JS, Marshall M, Fei Y, Roy Jackson W, Chaffee AL (2023) Comparison between reaction products obtained from the pyrolysis of marine and lacustrine kerogens. Fuel 337:126839

Ariskina K, Galliéro G, Obliger A (2024) Adsorption-induced swelling impact on CO2 transport in kerogen microporosity described by free volume theory. Fuel 359:130475

Baudin F, Jovovic I, Adam P, Ader M, Arnaud F, Gelin F et al (2024) Early stages of type I-S kerogen formation revealed by rock-eval 7S analysis of sediment from a modern halo-alkaline lake (Dziani Dzaha, Mayotte). Org Geochem 195:104794

Bonnaud PA, Oulebsir F, Galliero G, Vermorel R (2023) Modeling competitive adsorption and diffusion of CH4/CO2 mixtures confined in mature type-II kerogen: insights from molecular dynamics simulations. Fuel 352:129020

Burnham AK (2019) Kinetic models of vitrinite, kerogen, and bitumen reflectance. Org Geochem 131:50–59

Cai Y, Zhang X, Zou Y (2007) Dissolution—a new way to study the initial transportation of petroleum. Geochemistry 351–356

Fan D, Yang C, Sun H, Yao J, Zhang L, Jia C et al (2025) A framework of parallel physics-informed neural network with laplace transform for well testing interpretation. Phys Fluids 37:014114

Gama J, Schwark L (2023) Assessment of kerogen types and source rock potential of lower jurassic successions in the mandawa basin, SE Tanzania. Marine Petrol Geol 157:106505

Gong H, Jiang Z, Gao Z, Zhang F, Li T, Su S et al (2021) Innovative standard for graded evaluation of oil enrichment of lacustrine shale: a case study of the lower third member of the shahejie formation, zhanhua sag, eastern China. Energy Fuels 35:17698–17710

Hang J (2015) Source rock characteristics and hydrocarbon expulsion potential of the Middle Eocene Wenchang formation in the Huizhou depression, Pearl River Mouth basin, south China sea. Mar Pet Geol 67:635–652

Hazra B, Singh DP, Chakraborty P, Singh PK, Sahu SG, Adak AK (2021) Using rock-eval S4Tpeak as thermal maturity proxy for shales. Mar Pet Geol 127:104977

Hu T, Pang X, Jiang S, Wang Q, Zheng X, Ding X et al (2018a) Oil content evaluation of lacustrine organic-rich shale with strong heterogeneity: a case study of the Middle Permian Lucaogou Formation in Jimusaer Sag, Junggar Basin, NW China. Fuel 221:196–205

Hu T, Pang X, Jiang S, Wang Q, Xu T, Lu K et al (2018b) Impact of paleosalinity, dilution, redox, and paleoproductivity on organic matter enrichment in a saline lacustrine rift basin: A case study of paleogene organic-rich shale in Dongpu depression, Bohai bay basin, eastern China. Energy Fuels

Hu T, Pang X, Jiang F, Wang Q, Liu X, Wang Z et al (2021a) Movable oil content evaluation of lacustrine organic-rich shales: methods and a novel quantitative evaluation model. Earth-Sci Rev 214:103545

Hu T, Pang X, Jiang F, Wang Q, Wu G, Liu X et al (2021b) Key factors controlling shale oil enrichment in saline lacustrine rift basin: implications from two shale oil wells in Dongpu Depression, Bohai Bay Basin. Pet Sci 18

Hu T, Wu G, Xu Z, Pang X, Liu Y, Yu S (2022) Potential resources of conventional, tight, and shale oil and gas from paleogene wenchang formation source rocks in the huizhou depression. Adv Geo-Energy Res 6:402–414

Hu T, Liu Y, Jiang F, Pang X, Wang Q, Zhou K et al (2024a) A novel method for quantifying hydrocarbon micromigration in heterogeneous shale and the controlling mechanism. Energy 288:129712

Hu T, Jiang F, Pang X, Liu Y, Wu G, Zhou K et al (2024b) Identification and evaluation of shale oil micro-migration and its petroleum geological significance. Pet Explor Dev 51:127–140

Huang D, Li J, Zhang D (1984) Validity, limitations, and relevance of kerogen types and their classification parameters. J Sediment 18–33:135–136

Jarvie DM (2012) Shale resource systems for oil and gas: part 2: Shale-oil resource systems. Shale reservoirs-giant resources for the 21st century. AAPG Mem 97:89–119

Jiang QG, Lai MZ, Qian MH, Li ZM, Li Z, Huang ZK et al (2016) Quantitative characterization techniques and application studies of shale oil in different endowment states. Petrol Exp Geol 38:842–849

Jiang F, Chen D, Zhu C, Ning K, Ma L, Xu T et al (2022) Mechanisms for the anisotropic enrichment of organic matter in saline lake basin: a case study of the early eocene dongpu depression, eastern China. J Petrol Sci Eng 210:110035

Jiang F, Hu M, Hu T, Lyu J, Huang L, Liu C et al (2023) Controlling factors and models of shale oil enrichment in lower permian fengcheng formation, mahu sag, junggar basin. NW China Petrol Explor Dev 50:812–825

Johnson JR, Kobchenko M, Mondol NH, Renard F (2022) Multiscale synchrotron microtomography imaging of kerogen lenses in organic-rich shales from the norwegian continental shelf. Int J Coal Geol 253:103954

Li Q, Lu S, Li W, Hu Y, Zhang H, Zhang P (2015a) Hydrocarbon potential of shale and classification and evaluation criteria of shale oil from the Williston basin. Acta Geol Sin English Ed 89:198–199

Li W, Lu S, Xue H, Zhang P, Hu Y (2015b) Oil content in argillaceous dolomite from the Jianghan Basin, China: Application of new grading evaluation criteria to study shale oil potential. Fuel 143:424–429

Li S, Hu S, Xie X, Lv Q, Huang X, Ye J (2016) Assessment of shale oil potential using a new free hydrocarbon index. Int J Coal Geol 156:74–85

Li G, Zhu R, Zhang Y, Chen Y, Cui J, Jiang Y et al (2022) Geological characteristics, evaluation criteria and discovery significance of paleogene yingxiongling shale oil in qaidam basin, NW China. Petrol Explor Dev 49:21–36

Li Q (2021) Evaluation of Shale Oil and Gas Resource Potential of Typical Basins in the United States. Master's thesis. China University of Petroleum (East China)

Lis GP, Mastalerz M, Schimmelmann A, Lewan MD, Stankiewicz BA (2005) FTIR absorption indices for thermal maturity in comparison with vitrinite reflectance R0 in type-II kerogens from devonian black shales. Org Geochem 36:1533–1552

Liu H, Bao Y, Lai M, Li Z, Wu L, Zhu R et al (2024) Exploration of geochemical evaluation parameters for shale oil enrichment mobility-examining the shales of the Bakken Formation in the Williston Basin and the Paleoproterozoic Shahajie Formation of the Jiyang Pass in the Bohai Bay Basin as examples. Oil Gas Geol 45:622–636

Lu S, Huang W, Chen F, Li J, Wang M, Xue H et al (2012) Classification and evaluation criteria of shale oil and gas resources: discussion and application. Pet Explor Dev 39:268–276

Michael GE, Packwood J, Holba A (2013) Determination of in-situ hydrocarbon volumes in liquid rich shale plays. Unconventional Resources Technology Conference, Denver, Colorado, USA, 8

Milkov AV (2015) Risk tables for less biased and more consistent estimation of probability of geological success (PoS) for segments with conventional oil and gas prospective resources. Earth-Sci Rev 150:453–476

Moine E cheikh, Groune K, El Hamidi A, Khachani M, Halim M, Arsalane S (2016) Multistep process kinetics of the non-isothermal pyrolysis of Moroccan Rif oil shale. Energy 115:931–941

Pang X, Li M, Li B, Wang T, Hui S, Liu Y et al (2023) Main controlling factors and movability evaluation of continental shale oil. Earth-Sci Rev 243:104472

Patel R, Cunha P, Lan S, Xie KY (2024) Femtosecond laser ablation responses of kerogen-rich, argillaceous, and bituminous shale rocks. Geoenergy Sci Eng 240:213047

Peters KE (1986) Guidelines for evaluating petroleum source rock using programmed pyrolysis. Bulletin 70:318–329

Romero-Sarmiento MF, Rohais S, Littke R (2019) Lacustrine type I kerogen characterization at different thermal maturity levels: application to the late cretaceous Yacoraite formation in the Salta basin—Argentina. Int J Coal Geol 203:15–27

Rosenberg YO, Reznik IJ (2021) Evaluating transformation of marine kerogens from rock-eval measurements: A. Derivation of a scaled thermal maturation path from laboratory maturation data. Organic Geochem 162:104305

Safaei-Farouji M, Liu B, Gentzis T, Wen Z, Ma Z, Bai L et al (2023) Geochemical evolution of kerogen type III during hydrous pyrolysis: a case study from the damoguaihe formation, hailar basin, China. Geoenergy Sci Eng 228:211947

Salter TL, Watson JS, Sephton MA (2023) Effects of minerals (phyllosilicates and iron oxides) on the responses of aliphatic hydrocarbon containing kerogens (type I and type II) to analytical pyrolysis. J Anal Appl Pyrol 170:105900

Shao X, Pang X, Li H, Hu T, Xu T, Xu Y et al (2018) Pore network characteristics of lacustrine shales in the Dongpu Depression, Bohai Bay Basin, China, with implications for oil retention. Mar Pet Geol 96:457–473

Shao X, Song Y, Jiang L, Ma X, Jiang Z (2024) Graded evaluation and controls on in situ oil content within lacustrine shale of the upper cretaceous qingshankou formation, songliao basin, China. Energy Fuels 38:12925–12937

Siddiqui MAQ, Ali S, Fei H, Roshan H (2018) Current understanding of shale wettability: a review on contact angle measurements. Earth-Sci Rev 181:1–11

Teng J, Qiu L, Zhang S, Ma C (2022) Origin and diagenetic evolution of dolomites in paleogene shahejie formation lacustrine organic shale of jiyang depression, bohai bay basin, east China. Pet Explor Dev 49:1251–1265

Thakur DS, Wilkins ES, Nuttall HE (1984) Thermal degradation of shale oils: 1. Kinetics of vapour phase oil degradation. Fuel 63:401–407

Tissot BP, Welte DH (1978) Petroleum formation and occurrence. Springer, Berlin

Tissot BP, Welte DH (1984) Petroleum formation and occurrence. Springer, Berlin

Tissot BP, Pelet R, Ungerer PH (1987) Thermal history of sedimentary basins, maturation indices, and kinetics of oil and gas Generation1. AAPG Bull 71:1445–1466

Villalba D (2023) Characteristics of oils and their potential source rocks from the cherokee platform, oklahoma. Mar Petrol Geol 157:106457

Wang E, Li C, Feng Y, Song Y, Guo T, Li M et al (2022) Novel method for determining the oil moveable threshold and an innovative model for evaluating the oil content in shales. Energy 239:121848

Wu Y, Jiang F, Hu T, Xu Y, Guo J, Xu T et al (2024) Shale oil content evaluation and sweet spot prediction based on convolutional neural network. Mar Pet Geol 167:106997

Wu Y, Hu T, Jiang F, Guo J, Wang F, Qi Z, Huang R, Fang Z, Zheng X, Chen D (2025a) Lacustrine records of Paleocene-Eocene Thermal Maximum (PETM) triggered by volcanic activity. Org Geochem 200:104899

Wu Y, Jiang F, Xu Y, Guo J, Xu T, Hu T, Shen W, Zheng X, Chen D, Jiang Q, Yu S (2025b) Middle Eocene Climatic Optimum drove palaeoenvironmental fluctuations and organic matter enrichment in lacustrine facies of the Bohai Bay Basin, China. Palaeogeogr Palaeoclimatol Palaeoecol 659:112665

Xian Z, Xiu G, Feng M, Wen Z, Zhan N, Wei Z et al (2021) Quantitative method for evaluating shale oil resources based on movable oil content. Geofluids 2021:5554880

Yang M, Zuo Y, Yan KN, Zhou Y, Zhang Y, Zhang C (2022) Hydrocarbon generation history constrained by thermal history and hydrocarbon generation kinetics: a case study of the dongpu depression, bohai bay basin, China. Pet Sci 19:472–485

Yao J, Ding Y, Sun H, Fan D, Wang M, Jia C (2023) Productivity analysis of fractured horizontal wells in tight gas reservoirs using a gas–water two-phase flow model with consideration of a threshold pressure gradient. Energy Fuels 37:8190–8198

Zhang Y, Zeng J, Guo J (2009) Experimental simulation of feldspar dissolution under low temperature. Geol Rev 55:134–142

Zhang J, Lin L, Li Y, Tang X, Zhu L, Xing Y et al (2012) Shale oil classification and evaluation. Geol Front 19:322–331

Zhou J, Pang X (2002) Exploration and application of a method for calculating hydrocarbon production and discharge. Petrol Explor Dev 24–27

Zhu C, Jiang F, Zhang P, Zhao Z, Chen X, Wu Y et al (2023) Effect of petroleum chemical fraction and residual oil content in saline lacustrine organic-rich shale: a case study from the paleogene dongpu depression of north China. Pet Sci 20:649–669

Authors and Affiliations

Zhiming Xiong[1,2] · Tao Hu[1,2] · Yuqi Wu[1,2] · Yunlong Xu[3] · Jiyou Fu[4] · Huiyi Xiao[1,2] · Yuan Liu[1,2] · Kuo Zhou[1,2] · Qinglong Lei[1,2] · Tianshun Chen[1,2] · Xiaofei Lin[1,2] · Mingxing Liu[1,2] · Shu Jiang[5] · Maowen Li[6]

✉ Tao Hu
thu@cup.edu.cn

✉ Maowen Li
limw.syky@sinopec.com

[1] State Key Laboratory of Petroleum Resources and Engineering, China University of Petroleum (Beijing), Beijing 102249, China

[2] College of Geosciences, China University of Petroleum (Beijing), Beijing 102249, China

[3] Exploration and Development Research Institute, Zhongyuan Oilfield Company, SINOPEC, Puyang 457001, China

[4] Changqing Oilfield Shale Oil Development Branch, Xi'an 745000, China

[5] Key Laboratory of Tectonics and Petroleum Resources (China University of Geosciences), Ministry of Education, Wuhan 434100, China

[6] State Key Laboratory of Shale Oil and Shale Gas Resources and Effective Development, Sinopec Petroleum Exploration and Production Research Institute, Beijing 100083, China